IARJSET ISSN (O) 2393-8021, ISSN (P) 2394-1588

International Advanced Research Journal in Science, Engineering and Technology

Impact Factor 8.311 ⁜ Peer-reviewed & Refereed journal ⁜ Vol. 13, Issue 10, October 2026

DOI: 10.17148/IARJSET.2026.131066

Optimization of Electrostatic Precipitator Parameters Using the Taguchi Method

Mukilan K G[1], T. Pushparaj[2]

M.E. Thermal Engineering, Kings College of Engineering, Thanjavur, Tamil Nadu[1,2]

Abstract: Electrostatic precipitators (ESPs) are widely used for particulate control in industrial gas-cleaning systems, and their collection performance is influenced by applied voltage, volumetric gas flow rate and particle size. The present Phase-I study investigates these three parameters using a Taguchi L9 orthogonal array together with a literature-supported analytical collection model. The selected levels are 6, 9 and 12 kV for applied voltage, 0.05, 0.10 and 0.15 m^3/s for volumetric gas flow rate, and 2.5, 4 and 10 µm for particle size. The collection efficiency for each of the nine trials is calculated using the Deutsch–Anderson equation. A collecting area of 0.06 m^2 is adopted from a published wire-plate ESP geometry, while the effective particle migration velocity is estimated using the explicit screening relationship adopted for this Phase-I analytical study. The resulting responses are evaluated using the larger-the-better signal-to-noise ratio, response-level averages and ANOVA. The analysis identifies 12 kV applied voltage, 0.05 m^3/s gas flow rate and 2.5 µm particle size as the optimum combination within the selected levels. Particle size is ranked as the most influential factor, followed by gas flow rate and applied voltage. The present work therefore provides a quantitative baseline for ESP parameter optimization without claiming CFD simulation or experimental testing. In Phase-II, the optimized condition will be taken forward for higher-fidelity numerical and/or experimental validation, with additional parameters such as electrode spacing, discharge-electrode geometry, corona current, gas temperature and particle properties considered to improve the predictive capability and practical applicability of the ESP performance assessment.

Keywords: Electrostatic precipitator; Taguchi method; L9 orthogonal array; collection efficiency; applied voltage; volumetric gas flow rate; particle size; Deutsch–Anderson equation; ANOVA; optimization.

1. INTRODUCTION

Electrostatic precipitation is an important particulate-control technology used in industrial gas streams. The basic principle is to charge suspended particles electrically and drive the charged particles towards collecting electrodes by an electric field. The technology is attractive for large gas volumes because collection can be achieved with relatively low pressure loss compared with many mechanical filtration arrangements [1-3].

ESP performance is not governed by a single operating variable. Applied voltage changes the electric field and particle charging behaviour, while gas flow rate affects residence time and the aerodynamic transport of particles [1,6,10,11]. Particle size also influences charging, migration and the probability of reaching the collecting surface [2,3,7]. Recent ESP studies have therefore examined electrical conditions, electrode arrangement, gas distribution, particle transport and optimization methods[8-9,12-16].

The principal reference selected for this work is the 2026 study by Gwon et al. [1]. That work numerically investigated ESP collection performance and considered applied voltages of 6, 9 and 12 kV, volumetric flow rates of 0.05, 0.10 and 0.15 m^3/s and particle sizes of 10, 4 and 2.5 µm. These ranges are adopted as the factor levels of the present Taguchi study. The present work does not reproduce the CFD or artificial-neural-network methodology of that paper; instead, it uses an analytical model supported by the ESP performance literature [2-5].

A conventional three-factor, three-level full factorial study would require 27 combinations. The Taguchi L9 orthogonal array reduces the required combinations to nine while maintaining balanced representation of the three levels. Statistical and optimization-based ESP studies have demonstrated the value of structured parameter screening and optimization before detailed numerical or experimental validation [14,16,17,19,24]. This makes the method suitable for a preliminary engineering optimization in which the objective is to identify influential parameters and a promising operating combination before undertaking more expensive simulation or experimentation.

© IARJSET This work is licensed under a Creative Commons Attribution 4.0 International License

IARJSET ISSN (O) 2393-8021, ISSN (P) 2394-1588

International Advanced Research Journal in Science, Engineering and Technology

Impact Factor 8.311 ⁜ Peer-reviewed & Refereed journal ⁜ Vol. 13, Issue 10, October 2026

DOI: 10.17148/IARJSET.2026.131066

1.1 Problem statement

The problem addressed in this study is the identification of the relative influence of applied voltage, volumetric gas flow rate and particle size on ESP collection efficiency within the selected literature-based ranges. The work also seeks to determine an optimum combination of these factors using the Taguchi method.

1.2 Objectives

- To select three ESP operating parameters and three levels for each parameter.
- To construct an L9 orthogonal array for the selected factors.
- To calculate collection efficiency for the nine analytical trials.
- To evaluate the larger-the-better signal-to-noise ratio.
- To determine the factor-level response and contribution using ANOVA.
- To identify the optimum parameter combination.
- To establish a basis for Phase-II numerical or experimental validation.

1.3 Scope of the work

The study is limited to the three selected factors. Electrode geometry, electrode spacing, corona current, gas temperature, humidity, particle resistivity and re-entrainment are not independently optimized in Phase I. The response values are analytical/model-based values and are not experimental measurements.

2. LITERATURE REVIEW

Recent literature shows that ESP research continues to address collection efficiency, particle charging, electrode configuration, gas distribution, power consumption and numerical optimization. The following review focuses on work that is directly relevant to the three-factor screening strategy adopted in the present study.

[1] Gwon et al. (2026) numerically investigated ESP collection performance and used applied voltage, volumetric flow rate and particle size ranges that directly provide the operating levels adopted in this work.

[2] Badran and Mansour (2022) evaluated ESP performance indices and discussed analytical collection-efficiency relationships, supporting the use of the Deutsch–Anderson framework.

[3] A 2022 wire-plate ESP study combined numerical simulation and analytical evaluation of particle collection, demonstrating the relationship between gas flow, electric forces and particle migration.

[4] Andrade and Guerra (2025) investigated a single-stage wire-plate ESP and reported two collecting plates of 0.30 m × 0.10 m, providing the literature basis for the 0.06 m² collecting area used here.

[5] Abdykadyrov et al. (2026) modelled an advanced ESP power-supply system and reported drift-velocity magnitudes useful for establishing the order of magnitude of the migration-velocity screening calculation.

[6] Kim et al. (2022) evaluated a pilot-scale wet ESP and demonstrated the importance of operating conditions in practical particle collection.

[7] Moore et al. (2023) investigated ESP collection efficiency using atmospheric radon progeny as aerosol analogues, illustrating the application of ESPs to particulate collection measurements.

[8] A 2023 Journal of Electrostatics study investigated discharge-electrode effects and collection performance, highlighting the importance of electrode configuration in ESP operation.

[9] A 2023 study examined collection efficiency and ozone generation for different electrode arrangements, showing that electrical operating conditions must be considered together with collection performance.

[10] Zhang et al. (2024) investigated ESP performance using numerical and experimental approaches and reported the influence of operating and geometric conditions on collection behaviour.

[11] Ning et al. (2024) investigated electrostatic precipitation and particle removal characteristics, providing further evidence that electrical conditions and particle properties influence collection.

[12] A 2024 Fuel study examined the influence of temperature and magnetic-field-related conditions on ESP particle collection, illustrating the additional variables that may be considered in later stages.

[13] Cornette et al. (2024) evaluated a commercial ESP integrated with a small-scale wood-chip boiler and demonstrated practical particle-removal performance under real operating conditions.

[14] Hwang et al. (2025) optimized discharge-electrode shape in an ESP and combined numerical analysis with experimental verification, showing the value of staged optimization followed by validation.

[15] A 2025 Chemical Engineering Science study evaluated particle mass-transfer rates and provides useful context for interpreting transport and collection behaviour.

[16] Feng et al. (2026) developed a mathematical model and systematic optimization strategy for a two-stage ESP, demonstrating the usefulness of analytical and optimization methods before detailed validation.

[17] Nokpho et al. (2026) used CFD-EHD simulation and a full factorial design to rank wire-configuration variables, illustrating how statistical design can complement multiphysics modelling.

© IARJSET This work is licensed under a Creative Commons Attribution 4.0 International License

IARJSET ISSN (O) 2393-8021, ISSN (P) 2394-1588

International Advanced Research Journal in Science, Engineering and Technology

Impact Factor 8.311 ⁜ Peer-reviewed & Refereed journal ⁜ Vol. 13, Issue 10, October 2026

DOI: 10.17148/IARJSET.2026.131066

[18] Meng et al. (2026) numerically simulated and structurally optimized ESP configurations for particle purification, showing the current direction toward coupled flow, electric-field and particle-transport analysis.
[19] Shen et al. (2026) combined an artificial neural network with multi-objective optimization to balance ESP collection efficiency and energy consumption, demonstrating a more advanced optimization route for future work.
[20] Dudani and Takahama (2022) designed and fabricated an ESP for particle collection for infrared spectroscopy, providing experimental evidence for practical ESP construction and measurement.
[21] Wang et al. (2025) investigated a coated ESP for particulate removal and examined operating and geometric variables affecting collection performance.
[22] A 2025 theoretical and experimental study characterized a single-wire, single-stage ESP and emphasized the need for analytical theory together with experimental validation.
[23] A 2026 study investigated channel geometry and its influence on electrohydrodynamic processes and particle transport in ESPs, emphasizing gas distribution effects.
[24] A 2026 study developed a two-stage ESP optimization framework for ultrafine-particle removal and demonstrated the importance of applied voltage, inlet flow and charging/collection-zone design.
[25] A 2026 review discussed the development of ESPs toward smart, energy-aware systems and identified adaptive control and multi-objective optimization as future research directions.

2.1 Research gap

The reviewed studies show that detailed ESP research increasingly uses CFD, electrohydrodynamic coupling, experimental facilities, artificial intelligence and multi-objective optimization. Such methods are valuable, but they also require more computational or experimental resources. The present Phase-I work therefore focuses on a transparent L9 Taguchi framework combined with an analytical collection model. The intention is to identify the dominant variables and establish an optimum screening condition that can later be validated using higher-fidelity methods.

3. METHODOLOGY

3.1 Overall procedure

The methodology consists of six main stages: selection of factors and levels; construction of the L9 orthogonal array; estimation of effective particle migration velocity; calculation of collection efficiency; statistical analysis using S/N ratio and ANOVA; and confirmation of the optimum combination.

3.2 Input parameters and levels

Parameter	Level 1	Level 2	Level 3
Applied Voltage	6 kV	9 kV	12 kV
Gas Flow Rate	0.05 m^3/s	0.10 m^3/s	0.15 m^3/s
Particle Size	2.5 µm	4 µm	10 µm

The gas-flow factor is expressed as volumetric gas flow rate throughout the manuscript. It is not converted to gas velocity because the selected base-paper range is being used directly.

3.3 L9 orthogonal array

Run	Applied Voltage	Gas Flow Rate	Particle Size
1	1	1	1
2	1	2	2
3	1	3	3
4	2	1	2
5	2	2	3
6	2	3	1
7	3	1	3
8	3	2	1
9	3	3	2

© IARJSET This work is licensed under a Creative Commons Attribution 4.0 International License

IARJSET ISSN (O) 2393-8021, ISSN (P) 2394-1588

International Advanced Research Journal in Science, Engineering and Technology

Impact Factor 8.311 ⁜ Peer-reviewed & Refereed journal ⁜ Vol. 13, Issue 10, October 2026

DOI: 10.17148/IARJSET.2026.131066

3.4 Actual L9 experimental-design matrix

Run	Voltage (kV)	Flow rate (m³/s)	Particle size (µm)
1	6	0.05	2.5
2	6	0.10	4
3	6	0.15	10
4	9	0.05	4
5	9	0.10	10
6	9	0.15	2.5
7	12	0.05	10
8	12	0.10	2.5
9	12	0.15	4

The term experimental-design matrix is used here to describe the designed trials; the resulting response values themselves are analytical rather than measured.

3.5 Collection-efficiency equation

The Deutsch–Anderson relationship is used to estimate collection efficiency:

$$\eta = [1 - \exp(-A\, w_d / Q)] \times 100$$

For the present calculations, the collecting area is substituted directly into the equation as requested for the project calculation sheet:

$$\eta = [1 - \exp\{-(0.06 \times w_d / Q)\}] \times 100$$

where η is collection efficiency (%), w_d is effective particle migration velocity (m/s), Q is volumetric gas flow rate (m³/s), and 0.06 m² is the collecting area adopted from the published wire-plate geometry in [4].

3.6 Collecting-area basis

The collecting area used in the calculation is 0.06 m². Andrade and Guerra [4] report two collecting plates with dimensions of 30 cm × 10 cm. Therefore, the combined collecting area is 2 × (0.30 × 0.10) = 0.06 m². This is used as a literature-based modelling input; it is not claimed to be the exact physical geometry of the 2026 base paper.

3.7 Effective migration velocity

Because the Phase-I study does not use CFD or direct particle-charge measurements, an explicit proportional screening relationship is used:

$$w_d = 0.05 \times (V/10) \times (10/d_p)$$

The baseline magnitude is anchored to drift-velocity values reported in [5]. The proportional form is an assumption introduced for the present screening calculation. It must therefore be described in the manuscript as a modelling assumption and not as a universally established published correlation.

3.8 Calculation example

For Run 1, the selected values are V = 6 kV, Q = 0.05 m³/s and d_p = 2.5 µm. The migration velocity becomes w_d = 0.05 × (6/10) × (10/2.5) = 0.12 m/s. Substitution into the Deutsch–Anderson equation gives a collection efficiency of approximately 13.41%.

© IARJSET This work is licensed under a Creative Commons Attribution 4.0 International License

IARJSET ISSN (O) 2393-8021, ISSN (P) 2394-1588

International Advanced Research Journal in Science, Engineering and Technology

Impact Factor 8.311 ⁜ Peer-reviewed & Refereed journal ⁜ Vol. 13, Issue 10, October 2026

DOI: 10.17148/IARJSET.2026.131066

4. RESULTS AND DISCUSSION

4.1 Complete response calculation table

Run	V (kV)	Q (m^3/s)	d_p (µm)	w_d (m/s)	Collection Efficiency (%)
1	6	0.05	2.5	0.1200	13.41
2	6	0.10	4	0.0750	4.40
3	6	0.15	10	0.0300	1.19
4	9	0.05	4	0.0675	12.63
5	9	0.10	10	0.0450	2.66
6	9	0.15	2.5	0.1800	6.95
7	12	0.05	10	0.0600	6.95
8	12	0.10	2.5	0.2400	13.41
9	12	0.15	4	0.1500	5.82

The calculated collection efficiency ranges from 1.19% to 13.41%. The response is highest for the combinations that provide relatively high migration velocity and low gas flow rate. The response is lowest for the combination of low voltage, high gas flow rate and large particle size in the adopted screening model.

4.2 S/N ratio calculation table

Run	Collection Efficiency (%)	S/N Ratio (dB)
1	13.41	22.55
2	4.40	12.87
3	1.19	1.51
4	12.63	22.03
5	2.66	8.50
6	6.95	16.84
7	6.95	16.84
8	13.41	22.55
9	5.82	15.30

The larger-the-better characteristic is selected because higher collection efficiency is desirable. For one response per trial, the expression reduces to S/N = 20 log10(y), where y is the numerical collection efficiency expressed in percent.

4.3 S/N response table

Level	Applied Voltage	Gas Flow Rate	Particle Size
1	12.31	20.47	20.65
2	15.79	14.64	16.73
3	18.23	11.22	8.95
Delta	5.92	9.26	11.70
Rank	3	2	1

The response table gives the optimum level of each factor by selecting the highest S/N mean. Thus, applied voltage is optimum at Level 3 (12 kV), gas flow rate at Level 1 (0.05 m^3/s), and particle size at Level 1 (2.5 µm). The delta values give the influence ranking: particle size > gas flow rate > applied voltage.

4.4 Main-effects interpretation

The voltage S/N response rises from 12.31 dB at Level 1 to 18.23 dB at Level 3. This indicates that the higher applied-voltage level is favourable within the selected range. The gas-flow response falls from 20.47 dB to 11.22 dB, showing that the lowest selected flow rate is favourable. The particle-size response falls from 20.65 dB to 8.95 dB, giving the largest delta and therefore the strongest influence among the three factors.

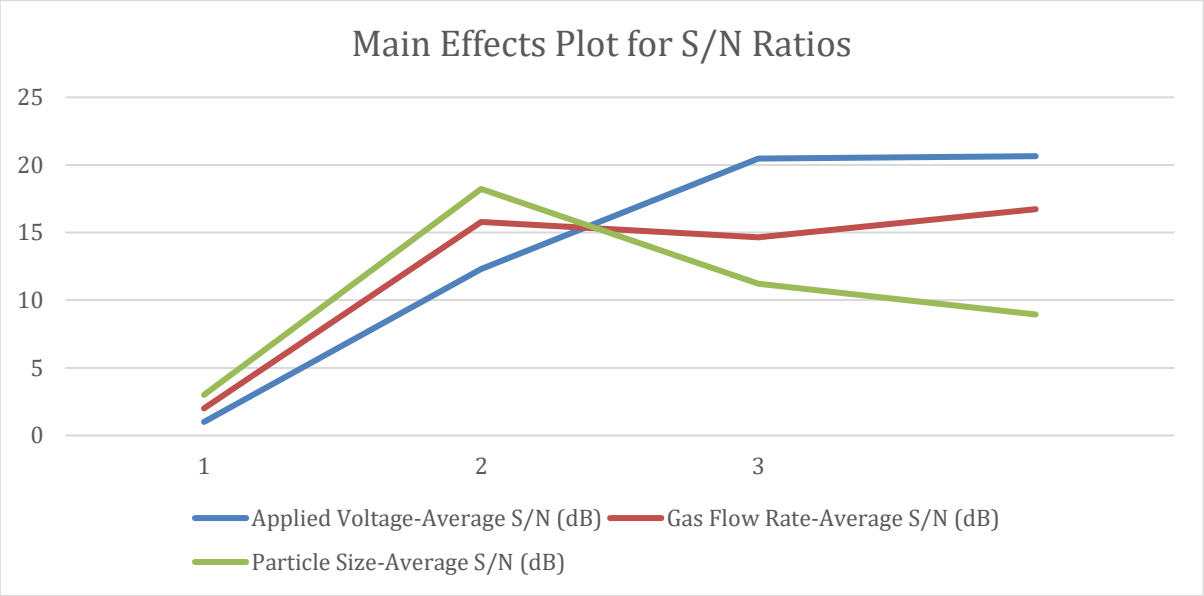
© IARJSET This work is licensed under a Creative Commons Attribution 4.0 International License

IARJSET ISSN (O) 2393-8021, ISSN (P) 2394-1588

International Advanced Research Journal in Science, Engineering and Technology

Impact Factor 8.311 ⁜ Peer-reviewed & Refereed journal ⁜ Vol. 13, Issue 10, October 2026

DOI: 10.17148/IARJSET.2026.131066



4.5 ANOVA results

Source	DF	SS	MS	F	Contribution (%)
Applied Voltage	2	53.1104	26.5552	1497.50	13.37
Gas Flow Rate	2	131.4329	65.7165	3705.88	33.08
Particle Size	2	212.7065	106.3533	5997.48	53.54
Error	2	0.0355	0.0177	—	0.01
Total	8	397.2852	49.6607	—	100.00

The ANOVA contribution ranking agrees with the S/N delta ranking. Particle size contributes the largest share, followed by gas flow rate and applied voltage. Because the responses originate from a deterministic analytical calculation, the ANOVA should be interpreted as a factor-contribution and ranking analysis. It should not be described as a replicated experimental significance test.

4.6 Optimum parameter combination

Parameter	Selected Level	Optimum Value
Applied Voltage	L3	12 kV
Gas Flow Rate	L1	0.05 m^3/s
Particle Size	L1	2.5 µm

The selected combination represents the best level of each factor within the L9 study according to the larger-the-better S/N criterion.

4.7 Confirmation calculation

Quantity	Value
Grand Mean S/N	15.44 dB
Predicted Optimum S/N	28.46 dB
Predicted Collection Efficiency	26.49 %
Confirmation S/N	27.97 dB
Confirmation Collection Efficiency	25.02 %
Change in S/N	−0.49 dB

© IARJSET This work is licensed under a Creative Commons Attribution 4.0 International License

IARJSET ISSN (O) 2393-8021, ISSN (P) 2394-1588

International Advanced Research Journal in Science, Engineering and Technology

Impact Factor 8.311 ⁜ Peer-reviewed & Refereed journal ⁜ Vol. 13, Issue 10, October 2026

DOI: 10.17148/IARJSET.2026.131066

The predicted optimum is obtained from the grand mean and the selected optimum level effects. The confirmation value in the project dataset is 27.97 dB, corresponding to 25.02% collection efficiency. The difference of −0.49 dB is treated as a confirmation difference within the model-based study and is not presented as experimental measurement error.

4.8 Engineering discussion

The observed ranking follows the structure of the adopted analytical model. Particle size has the largest effect because the migration-velocity screening relationship includes an inverse particle-size term. Gas flow rate has the next largest effect because it appears in the denominator of the Deutsch–Anderson exponent. Applied voltage increases the estimated migration velocity and therefore improves the calculated collection efficiency within the selected range.

Actual ESP systems may show additional behaviour that is not represented by this simplified calculation. Corona onset, space charge, particle charging mechanisms, electric-field non-uniformity, temperature, humidity and re-entrainment can modify the measured response. The present results should therefore be used as a screening and optimization baseline rather than as a direct prediction of the performance of a particular industrial ESP.

4.9 Comparison with selected recent literature

Reference	Main method	Relevance to present work
Gwon et al. [1]	Numerical study + ANN	Provides the three operating ranges used as factor levels.
Badran & Mansour [2]	Analytical ESP performance	Supports the efficiency framework.
Andrade & Guerra [4]	Wire-plate ESP study	Provides collecting-area basis.
Abdykadyrov et al. [5]	ESP power-supply modelling	Supports drift-velocity order of magnitude.
Hwang et al. [14]	Simulation + experiment	Shows staged optimization and validation.
Feng et al. [16]	Mathematical optimization	Supports model-based optimization strategy.
Nokpho et al. [17]	CFD-EHD + factorial design	Demonstrates statistical factor ranking.
Meng et al. [18]	Multiphysics numerical optimization	Shows direction for Phase-II validation.
Wang et al. [24]	Numerical ESP optimization	Supports future extension to additional operating parameters.

4.10 Limitations

- The collection-efficiency values are model-based rather than experimentally measured.
- The migration-velocity relationship is an explicit project assumption used for screening.
- The 0.06 m² collecting area is adopted from a published geometry and is not claimed to reproduce the exact base-paper geometry.
- Only three factors are optimized in Phase I.
- The ANOVA error term is not equivalent to independent experimental repeatability.
- The optimum is conditional on the selected levels and assumptions.

4.11 Proposed Phase-II work

The next stage of the project will use the optimum condition identified in Phase I as the starting point for higher-fidelity validation. The preferred route is to replace the screening migration-velocity assumption with either CFD-EHD results or experimentally determined collection efficiency. The model can then be extended to electrode spacing, discharge-electrode diameter or configuration, gas temperature, corona current and particle properties. Repeated measurements or repeated numerical cases can also be used to obtain a more defensible experimental or computational error estimate.

© IARJSET This work is licensed under a Creative Commons Attribution 4.0 International License

IARJSET ISSN (O) 2393-8021, ISSN (P) 2394-1588

International Advanced Research Journal in Science, Engineering and Technology

Impact Factor 8.311 ⁜ Peer-reviewed & Refereed journal ⁜ Vol. 13, Issue 10, October 2026

DOI: 10.17148/IARJSET.2026.131066

5. CONCLUSION

A Taguchi L9 framework was applied to the analytical optimization of an electrostatic precipitator using applied voltage, volumetric gas flow rate and particle size as the selected parameters. The factor levels were taken from the operating range of the selected 2026 base study. Collection efficiency was evaluated using the Deutsch–Anderson equation with a collecting area of 0.06 m² and a transparent migration-velocity screening relationship.

The nine model-based responses range from 1.19% to 13.41%. The larger-the-better S/N analysis identifies 12 kV, 0.05 m³/s and 2.5 µm as the optimum combination within the selected ranges. Particle size is the most influential factor, followed by gas flow rate and applied voltage. The project dataset gives a predicted optimum S/N of 28.46 dB and predicted collection efficiency of 26.49%, followed by a confirmation value of 27.97 dB and 25.02%.

The main contribution of the Phase-I work is a compact, reproducible screening procedure that can be completed without CFD or a physical ESP test rig. The next phase will focus on validation and refinement. Higher-fidelity numerical or experimental work can be used to test the optimum combination, quantify uncertainty and investigate additional design and operating variables. This progression allows the present Taguchi study to serve as a practical starting point for continued ESP performance optimization.

5.1 Future scope

- Validate the optimum condition using experimental inlet and outlet particle concentrations.
- Replace the screening migration-velocity assumption with CFD-EHD or measured particle migration data.
- Investigate electrode spacing, discharge-electrode diameter and electrode configuration.
- Study the effects of gas temperature, humidity and particle resistivity.
- Include pressure drop and power consumption as additional performance responses.
- Compare Taguchi optimization with response-surface, genetic-algorithm and multi-objective methods.

REFERENCES

[1]. Gwon, J. G., Choi, H. Y., Seo, Y. M., Choi, H. K., & Park, Y. G. (2026). Collection performance of electrostatic precipitators with diagonal wire-line angles: A numerical study and prediction using artificial neural networks. Powder Technology, 475, 122321. DOI: 10.1016/j.powtec.2026.122321.

[2]. Badran, M., & Mansour, A. M. (2022). Evaluating Performance Indices of Electrostatic Precipitators. Energies, 15(18), 6647. DOI: 10.3390/en15186647.

[3]. Numerical Simulation and Analytical Evaluation of the Collection Efficiency of the Particles in a Gas by the Wire-Plate Electrostatic Precipitators. (2022). Applied Sciences, 12(13), 6401. DOI: 10.3390/app12136401.

[4]. Andrade, R. G. S. A., & Guerra, V. G. (2025). Impact of Discharge Electrode Positioning on Nanoparticle Collection in a Single-Stage Wire-Plate Electrostatic Precipitator. ACS Omega, 10(24), 25467–25478. DOI: 10.1021/acsomega.5c00722.

[5]. Abdykadyrov, et al. (2026). Development and Modeling of an Advanced Power Supply System for Electrostatic Precipitators to Improve Environmental Efficiency. Designs, 10(2), 34. DOI: 10.3390/designs10020034.

[6]. Kim, M.-S., Jo, H., Park, Y., et al. (2022). Performance Evaluation of a Novel Pilot-Scale Wet Electrostatic Precipitator in a Bio-Drying-Assisted Solid Recovered Fuel Generation Plant. Sustainability, 14(14), 8702. DOI: 10.3390/su14148702.

[7]. Moore, M. E., Keillor, M. E., Kasparek, D. M., Day, A. R., & Glasgow, B. D. (2023). Electrostatic precipitator collection efficiency studies using atmospheric radon progeny as aerosol analogs for nuclear explosion radionuclides. Journal of Environmental Radioactivity, 270, 107306. DOI: 10.1016/j.jenvrad.2023.107306.

[8]. Study on influence of electrodes in an electrostatic precipitator. (2023). Journal of Electrostatics, 123, 103808. DOI: 10.1016/j.elstat.2023.103808.

[9]. Zukeran, A., et al. (2023). Effect of collection efficiency and reducing ozone generation in an electrostatic precipitator with knife edge disk type electrode. Journal of Electrostatics, 125, 103842. DOI: 10.1016/j.elstat.2023.103842.

[10]. Zhang, et al. (2024). Environmental Engineering Science, 41(4). DOI: 10.1089/ees.2023.0241.

[11]. Ning, et al. (2024). ACS Omega, 9(35), 37396–37407. DOI: 10.1021/acsomega.4c06500.

[12]. Influences of temperature and magnetic field on electrostatic precipitation. (2024). Fuel, 366, 131291. DOI: 10.1016/j.fuel.2024.131291.

[13]. Cornette, J. F. P., Dyakov, I. V., Plissart, P., Bram, S., & Blondeau, J. (2024). In-situ evaluation of a commercial electrostatic precipitator integrated in a small-scale wood chip boiler. Journal of Electrostatics, 128, 103897. DOI: 10.1016/j.elstat.2024.103897.

© IARJSET This work is licensed under a Creative Commons Attribution 4.0 International License

IARJSET ISSN (O) 2393-8021, ISSN (P) 2394-1588

International Advanced Research Journal in Science, Engineering and Technology

Impact Factor 8.311 ⁜ Peer-reviewed & Refereed journal ⁜ Vol. 13, Issue 10, October 2026

DOI: 10.17148/IARJSET.2026.131066

[14]. Hwang, S.-J., Lee, G.-H., Kim, H.-J., & Yook, S.-J. (2025). Discharge electrode shape optimization for the performance improvement of electrostatic precipitator with six-branched spike discharge electrode and hexagonal collecting plate. Powder Technology, 453, 120662. DOI: 10.1016/j.powtec.2025.120662.

[15]. Evaluation of particle mass transfer rates in an electrostatic precipitator. (2025). Chemical Engineering Science, 307, 121338. DOI: 10.1016/j.ces.2025.121338.

[16]. Feng, Z., Liu, S., Xie, J., Meng, C., Zhang, R., & Cao, S.-J. (2026). Highly-efficient removal of nanoparticles using two-stage electrostatic precipitators: Development of a mathematical model and systematic optimal design. Journal of Electrostatics, 139, 104219. DOI: 10.1016/j.elstat.2025.104219.

[17]. Nokpho, P., Tanprasert, S., Chalermsinsuwan, B., & Piemjaiswang, R. (2026). Effect of wire configuration on collection efficiency of an electrostatic precipitator using EHD simulation. Journal of Environmental Chemical Engineering, 14(5), 124274. DOI: 10.1016/j.jece.2026.124274.

[18]. Meng, L., Wang, H., Su, N., He, M., Mo, F., & Liu, C. (2026). Numerical simulation and structural optimization of electrostatic precipitators for particle purification in space capsules. Scientific Reports. DOI: 10.1038/s41598-026-74487-3.

[19]. Wang, J., Liu, X.-Y., Tan, Z.-P., Shen, X.-X., & Ma, J.-C. (2026). Optimization of guide-vane-enhanced longitudinal vortex electrostatic precipitators based on artificial neural network and non-dominated sorting genetic algorithm for balancing particulate matter collection and energy consumption. Particulate Science and Technology. DOI: 10.1080/02726351.2026.2732074.

[20]. Dudani, N., & Takahama, S. (2022). Design and fabrication of an electrostatic precipitator for infrared spectroscopy. Atmospheric Measurement Techniques, 15, 4693–4707. DOI: 10.5194/amt-15-4693-2022.

[21]. Wang, C., Yan, C., Zhang, Z., et al. (2025). A novel electrostatic precipitator with superhydrophobic coating for enhanced particulate removal efficiency restoration. Building Simulation, 18(8), 2057–2066. DOI: 10.1007/s12273-025-1299-6.

[22]. Theoretical and experimental studies on characterization and collection of particulate matter in single-wire, single-stage electrostatic precipitator with square cross-section. (2025). Journal of the Air & Waste Management Association. DOI: 10.1080/10962247.2025.2467666.

[23]. Kilic, H., Konuk Ege, G., Temiz, I., Genc, G., Akay Sefer, O., & Sefer, A. (2026). Effect of Channel Geometry on the Performance of an Electrostatic Precipitator: A Comparative Numerical Study. Applied Sciences, 16(9), 4356. DOI: 10.3390/app16094356.

[24]. Numerical optimization on two-stage electrostatic precipitator for high-efficiency removal of airborne ultrafine particles. (2026). Separation and Purification Technology, 396, 137980. DOI: 10.1016/j.seppur.2026.137980.

[25]. Li, J., Lu, Y., Xu, X., Sun, C., Zhu, Q., & Zhao, D. (2026). Electrostatic precipitators in the era of smart technology: Electrical efficiency, vibration mitigation, and noise reduction. Sound & Vibration, 60(5). DOI: 10.59400/sv4277.

Appendix A. Complete project calculation table

Run	V (kV)	Q (m³/s)	d_p (μm)	w_d (m/s)	A w_d/Q	η (%)	S/N (dB)
1	6	0.05	2.5	0.1200	0.1440	13.41	22.55
2	6	0.10	4	0.0750	0.0450	4.40	12.87
3	6	0.15	10	0.0300	0.0120	1.19	1.51
4	9	0.05	4	0.0675	0.0810	12.63	22.03
5	9	0.10	10	0.0450	0.0270	2.66	8.50
6	9	0.15	2.5	0.1800	0.0720	6.95	16.84
7	12	0.05	10	0.0600	0.0720	6.95	16.84
8	12	0.10	2.5	0.2400	0.1440	13.41	22.55
9	12	0.15	4	0.1500	0.0600	5.82	15.30

Appendix B. Parameter-level summary

Parameter	Level 1	Level 2	Level 3	Optimum	Rank
Applied Voltage	6 kV	9 kV	12 kV	12 kV	3
Gas Flow Rate	0.05 m³/s	0.10 m³/s	0.15 m³/s	0.05 m³/s	2
Particle Size	2.5 μm	4 μm	10 μm	2.5 μm	1

© IARJSET This work is licensed under a Creative Commons Attribution 4.0 International License

IARJSET ISSN (O) 2393-8021, ISSN (P) 2394-1588

International Advanced Research Journal in Science, Engineering and Technology

Impact Factor 8.311 ⁜ Peer-reviewed & Refereed journal ⁜ Vol. 13, Issue 10, October 2026

DOI: 10.17148/IARJSET.2026.131066

Appendix C. Statistical summary

Item	Result
S/N characteristic	Larger-the-better
Grand mean S/N	15.44 dB
Predicted optimum S/N	28.46 dB
Predicted efficiency	26.49 %
Confirmation S/N	27.97 dB
Confirmation efficiency	25.02 %
Change in S/N	−0.49 dB
Dominant factor	Particle Size
Overall ranking	Particle Size > Gas Flow Rate > Applied Voltage

© IARJSET This work is licensed under a Creative Commons Attribution 4.0 International License